HHS Public Access

Author manuscript

Nat Immunol. Author manuscript; available in PMC 2016 January 01.

Published in final edited form as:

Nat Immunol. 2015 July ; 16(7): 775–784. doi:10.1038/ni.3170.

Brg1 activates enhancer repertoires to establish B cell identity and modulate cell growth

Claudia Bossen[1], **Caroline S Murre**[1], **Aaron N Chang**[2], **Robert Mansson**[3], **Hans-Reimer Rodewald**[4], and **Cornelis Murre**[1]

[1]Department of Molecular Biology, University of California, San Diego, La Jolla, California, USA

[2]Center for Computational Biology, Institute for Genomic Medicine, University of California, San Diego, La Jolla, California, USA

[3]Center for Hematology and Regenerative Medicine, Karolinska Institute, Huddinge, Sweden

[4]Division of Cellular Immunology, German Cancer Research Center, Im Neuenheimer Field 280, Heidelberg, Germany

Abstract

Early B cell development is orchestrated by the combined activities of the transcriptional regulators E2A, EBF1, Foxo1 and Ikaros. However, how the genome-wide binding patterns of these regulators are modulated during B-lineage development remains to be determined. Here, we found that in lymphoid progenitors the chromatin remodeler Brg1 specified the B cell fate. In committed pro-B cells Brg1 regulated *Igh* locus contraction and controlled *Myc* expression to modulate the expression of genes that regulate ribosome biogenesis. In committed pro-B cells Brg1 suppressed a pre-B lineage-specific pattern of gene expression. Finally, we found that Brg1 acted mechanistically to establish B cell fate and modulate cell growth by facilitating access of lineage-specific transcription factors to poised enhancer repertoires.

Introduction

B cell differentiation is controlled by a subset of well-characterized transcription factors acting at distinct checkpoints during hematopoiesis. The first cells in the fetal liver or bone marrow that are primed for the B cell fate are the common lymphoid progenitors (CLPs). The transcriptional regulators PU.1 and Ikaros are essential for CLPs to develop[1, 2]. The CLP population is heterogeneous and can be segregated into two compartments based on the

Correspondence should be addressed to C.M. (murre@biomail.ucsd.edu).

Accession codes

Gene Expression Omnibus. ATAC-Seq, Brg1 and Ikaros ChIP-Seq, RNA-Seq: GSE66978

AUTHOR CONTRIBUTIONS

C.B. performed and analyzed the majority of the experiments. C.S.M. performed FISH experiments. A.N.C. analyzed RNA-Seq data. R.M. sorted developmental B cell stages. H.R.R. provided *Il7r*$^{Cre/+}$ mice. C.B. and C.M. wrote the manuscript. C.M. supervised the study.

COMPETING FINANCIAL INTERESTS

The authors declare no competing financial interests.

expression of the cell surface marker Ly6D. $Ly6D^-$ CLPs, termed ALPs (all-lymphoid progenitors), display B, T and NK lineage potential, whereas the $Ly6D^+$ CLPs, also named BLPs (B-cell biased lymphoid progenitors), mainly give rise to B-lineage cells[3, 4]. The E2A proteins control the developmental transition from ALPs to BLPs[3]. Once the E2A proteins are activated, they induce the expression of *Foxo1*, which in turn activates the expression of *Ebf1* (ref. 5). EBF1 and Foxo1 then act in a positive intergenic feedback loop to promote the B cell fate. Developmental progression from the pro-B to the pre-B cell stage is controlled by the pre-BCR. Once the pre-BCR is expressed on the cell surface, pro-B cells expand to give rise to large pre-B cells, which in turn differentiate into small resting pre-B cells. Both pro-B and large pre-B cells require c-Myc to promote cellular expansion, cell growth and cell survival[6, 7]. Ikaros is essential to promote the developmental transition from the large pre-B cell to the small pre-B cell stage[8–10].

The developmental progress of B cells can also be characterized by the status of immunoglobulin (Ig) gene rearrangement. The heavy chain (*Igh*) gene undergoes D_H-J_H recombination starting at the BLP stage, whereas V_H-D_HJ_H rearrangement occurs at the pro-B cell stage. Ig light chain recombination is initiated and completed at the small pre-B cell stage. Recombination of the Igh gene concurs with commitment to the B cell lineage and is tightly regulated to ensure that D_H-J_H recombination precedes V_H-D_HJ_H recombination and that the entire V_H repertoire is represented. The murine V_H repertoire is composed of over a hundred V_H segments divided across different families that are segregated into proximal and distal V_H segments[11]. During developmental progression, distal V_H segments are brought into closer spatial proximity of the J_H segments through locus contraction[12]. *Igh* locus contraction is controlled by multiple transcription factors including E2A, YY1 and Pax5 (refs. 13–15).

Lineage-specific transcriptional regulators such as E2A, EBF1 and Foxo1 act primarily by binding to distally located enhancer elements that are characterized by DNase I hypersensitivity, active histone marks and non-coding transcription[16]. Enhancers displaying H3K4me1, H3K4me2 and H3K27ac histone marks are considered active and are bound by the histone acetyltransferase p300 (ref. 17). On the other hand, enhancers without H3K27ac deposition are thought to be in a poised state[17]. Enhancers activate transcription by looping to their cognate promoter regions. Promoter-enhancer interactions are facilitated by the mediator or cohesin complexes[18]. Super-enhancers, representing clusters of enhancers, are frequently associated with developmentally regulated genes and are characterized by a high density of mediator and transcription factor binding[19]. Enhancer elements need to be established, maintained and/or inactivated during the developmental progression of cells. A key step for enhancer establishment is the removal of nucleosomes to allow transcription factor occupancy across enhancer regions. Prominent among chromatin remodelers that promote nucleosome depletion is the BAF (Brahma-associated factor) complex[20]. The BAF complex consists of at least 14 subunits encoded by 28 genes. The polymorphic composition of the BAF complex underlies its specialized functions in a tissue-specific manner. Nucleosome depletion requires the ATPase activity of the BAF complex members Brm or Brg1 encoded respectively by *Smarca2* and *Smarca4* (ref. 20).

Here, we demonstrate that Brg1 acts at multiple developmental stages to orchestrate B cell development. Specifically, we found that at the onset of B cell development, Brg1 provided transcriptional regulators closely associated with a B-lineage specific transcription signature access to a large enhancer repertoire. In committed pro-B cells, Brg1 was essential for accessibility across transcription factor binding sites across the *Igh* locus and concomitant merging of distal and proximal V_H regions. Finally, we demonstrate that Brg1 controls pro-B cell growth and prevents premature pre-B cell differentiation by permitting EBF1, Ikaros and Pax5 access to a distally located *Myc* super-enhancer. Taken together, these observations show how a lineage-specific chromatin remodeler specifies cell fate, regulates cell growth and enforces developmental checkpoints.

RESULTS

Brg1 specifies the B cell fate

Previous studies have indicated an important role for Brg1 in early B cell development[21–24]. However, it has remained unclear how Brg1 expression acts to orchestrate B cell fate. As a first approach to address this question, Brg1 expression was depleted in the CLP compartment using *Smarca4*$^{fl/fl}$ and *Il7r*$^{Cre/+}$ mice[25, 26]. To alleviate potential defects due to *Il7r* heterozygosity, we directly compared *Smarca4*$^{fl/fl}$*Il7r*$^{Cre/+}$ mice to *Smarca4*$^{fl/+}$*Il7r*$^{Cre/+}$ littermate control mice. *Smarca4*$^{fl/fl}$*Il7r*$^{Cre/+}$ mice did not display gross abnormalities and bone marrow (BM) cellularity was normal (Fig. 1a). B cell cellularity, however, was reduced more than ten-fold in *Smarca4*$^{fl/fl}$*Il7r*$^{Cre/+}$ mice as compared to control mice (Fig. 1b). In concordance with previous results, cellularity of the pro-B, pre-B, immature B and mature B cell compartments was greatly reduced in BMs derived from *Smarca4*$^{fl/fl}$*Il7r*$^{Cre/+}$ mice (Fig. 1c and Supplementary Fig. 1)[24]. In contrast, ALP and BLP cell numbers were not altered in *Smarca4*$^{fl/fl}$*Il7r*$^{Cre/+}$ mice as compared to control littermates (Fig. 1d). To determine whether B cells detected in *Smarca4*$^{fl/fl}$*Il7r*$^{Cre/+}$ mice were efficiently depleted for Brg1 expression, we crossed *Smarca4*$^{fl/fl}$*Il7r*$^{Cre/+}$ mice with mice containing the yellow fluorescent protein (YFP) inserted into the *Rosa26* locus. In *Rosa26*$^{YFP/+}$ mice, YFP expression is blocked by a *lox*P-flanked STOP site, which is removed in cells that express Cre recombinase. A large proportion of Ly6D$^+$ CLPs (>90%) displayed YFP expression indicative of efficient deletion in the BLP compartment (Fig. 1e). On the other hand, a substantial proportion of pro-B cells and pre-B cells lacked YFP expression in *Smarca4*$^{fl/fl}$*Il7r*$^{Cre/+}$*Rosa26*$^{YFP/+}$ mice suggesting that pro-B cells and pre-B cells that develop in *Smarca4*$^{fl/fl}$*Il7r*$^{Cre/+}$ mice are not completely abrogated for Brg1 expression (Fig. 1e).

To determine whether Brg1 expression in hematopoietic progenitors is required before and/or at the CLP cell stage, Brg1 expression was depleted using tamoxifen-inducible ER-Cre transgenic mice. To this end, CD45.2$^+$ *Smarca4*$^{+/+}$ER-Cre and *Smarca4*$^{fl/fl}$ER-Cre BM cells were injected with wild-type CD45.1$^+$ BM cells into CD45.1 recipient mice. Ten weeks post-transplantation, recipient mice were injected with tamoxifen and examined for the presence of CLPs. Treatment of the mice with tamoxifen resulted in a significant reduction of CLPs arising from Brg1-deficient (*Smarca4*$^{\Delta/\Delta}$) BM cells as compared to Brg1-proficient (*Smarca4*$^{+/+}$) BM cells (Supplementary Fig. 2a). BLPs were further reduced in the

absence of Brg1, and *Smarca4*$^{\Delta/\Delta}$ developing B cells were virtually undetectable (Supplementary Fig. 2a,b). Taken together, these observations indicate that Brg1 is required to establish the B cell fate.

Genome-wide Brg1 occupancy in pro-B cells

As a first approach to determine how Brg1 regulates pro-B cell development, we examined *Smarca4* transcript expression during hematopoiesis. For this purpose, RNA was isolated from LSK ($Lin^{-}Sca1^{+}Kit^{+}$), LMPP (lymphoid-primed multipotent progenitor), ALP, BLP, pro-B, pre-B, immature B and mature B cells and analyzed for *Smarca4* expression. We found the *Smarca4* transcript abundance was absent or low in the majority of hematopoietic progenitors but was elevated in BLPs (Fig. 2a). In committed B-lineage cells, *Smarca4* expression was highest in pro-B cells but declined in pre-B cells (Fig. 2a).

To determine the spectrum of Brg1-bound sites across the pro-B cell genome, we performed ChIP-Seq analysis using an antibody directed against Brg1. We found that Brg1 occupancy was abundant (13,000 bound sites) with the majority of Brg1 binding detected at putative enhancers (Fig. 2b,c). Brg1-bound sites were enriched across intergenic and intronic regions and were predominantly associated with genomic regions that displayed deposition of H3K4me1 and H3K4me2 (Fig. 2b,c). Brg1 also bound to promoter regions, albeit with much reduced frequencies when compared to putative enhancer elements (Fig. 2b,c). To evaluate the degree of overlap between Brg1 occupancy and an active enhancer repertoire, including super-enhancers, we compared Brg1-bound sites with p300 occupancy. Notably, a large fraction of Brg1-bound sites overlapped with p300 occupancy indicating that Brg1 primarily associates with an active enhancer repertoire (Fig. 2d). As expected, Brg1 occupancy was observed across enhancer elements that exhibited E2A and p300 binding and were associated with the expression of a subset of B-lineage specific genes, including *Pax5* and *Cd19* (Fig. 2e). At a genome-wide level, Brg1 occupancy was highly enriched for E2A, EBF1, IRF, Ikaros, PU.1 and Runx consensus binding motifs (Fig. 2f). Consistent with this analysis, Brg1 occupancy was closely associated with Ikaros occupancy and, to a lesser degree, with E2A-, EBF-, Pax5- and PU.1-bound sites (Fig. 2g). In contrast, Brg1-bound sites were not frequently associated with CTCF occupancy (Fig. 2g). Brg1 binding was observed at super-enhancers including the *Foxo1* and *Inpp5d* super-enhancers (Supplementary Fig. 3a). The proportion of Brg1 binding at super-enhancers was comparable to transcription factors known to associate with super-enhancers such as E2A and Pax5 and Med1, a member of the mediator complex (Supplementary Fig. 3b). To inspect the binding strength of Brg1 at super-enhancers, we normalized the number of tag counts by the size of the enhancers, since the median size of super-enhancers is approximately 10-fold larger than typical enhancers[19]. We found that, unlike Med1, Brg1 binding strength was not increased at super-enhancers when compared to typical enhancers (Supplementary Fig. 3c).

Previous studies have established that Ikaros interacts with Brg1 (refs. 27, 28). These findings raised the question as to whether Ikaros recruits Brg1 to the pro-B cell enhancer repertoire. Hence, we investigated Ikaros binding in B cell progenitors using E2A-deficient pre-pro-B cells[29]. We found that, in pre-pro-B cells, Ikaros bound to a spectrum of sites

distinct from that observed in pro-B cells even though the levels of Ikaros proteins were similar in both cell types (Supplementary Fig. 4a)[30]. Notably, the *de novo* enhancer repertoire associated with pro-B cells displayed overlapping patterns of Ikaros and Brg1 occupancy (Supplementary Fig. 4a). Furthermore, pro-B specific Brg1-bound sites were associated with regions that became depleted for nucleosomes during the transition from the pre-pro-B to the pro-B cell stage (Supplementary Fig. 4b). Collectively, these results show that Brg1 binding is closely associated with a *de novo* enhancer repertoire that is established during the pre-pro-B to the pro-B cell transition.

Brg1 facilitates access to enhancer repertoires

As Brg1 is a chromatin remodeler and is required to specify the B cell fate, we considered the possibility that Brg1 plays a crucial role in the generation of a *de novo* enhancer repertoire by depleting nucleosomes across an ensemble of B-lineage specific enhancers. The expression of genes associated with the establishment of B cell identity is activated in BLPs suggesting that a pro-B cell specific enhancer repertoire is established in the BLP compartment. As a first approach to explore this possibility, we used ATAC (assay for transposase-accessible chromatin) sequencing to capture open chromatin sites[31]. ATAC-Seq generates comparable results to DNase I hypersensitivity mapping and involves incubation of nuclei with a transposase. The transposase preferentially integrates into active regulatory regions and simultaneously fragments and tags the genome with sequencing adaptors. This technique can be used for small numbers of cells, including progenitor populations[31]. To identify accessible enhancer repertoires in B cell progenitors, ALPs and BLPs were sorted from *Smarca4*$^{fl/+}$*Il7r*$^{Cre/+}$ and *Smarca4*$^{fl/fl}$*Il7r*$^{Cre/+}$ mice. Sorted cells were incubated with transposase and sequenced at a global scale. Next, ATAC-Seq tag counts were plotted as a function of genomic separation from E2A-, Ikaros-, EBF1- and CTCF-bound sites (Fig. 3a). As expected, enhancer repertoires associated with E2A, Ikaros and EBF1 occupancy were more accessible to transposase activity in BLPs than in ALPs (Fig. 3a). These data indicate that at a developmental stage in which progenitors become specified to the B cell lineage, the enhancer repertoire associated with a B-lineage-specific program of gene expression becomes depleted for nucleosomes. In contrast, Brg1-deficient BLPs when compared to Brg1-proficient BLPs displayed either no increase or a reduced increase in the number ATAC reads for enhancer repertoires associated with E2A, Ikaros and EBF1 occupancy (Fig. 3a). Genomic regions associated with CTCF occupancy showed comparable ATAC tag counts in both Brg1-proficient and Brg1-deficient ALPs and BLPs (Fig. 3a). Since E2A and EBF1 directly regulate *Foxo1* expression in the BLP compartment, we examined whether nucleosomes were depleted across putative enhancers associated with the *Foxo1* locus[5]. We found that indeed, Brg1 expression was essential to evict nucleosomes across a distally located *Foxo1* enhancer associated with E2A and EBF1 occupancy (Fig. 3b; **left**). Likewise, Brg1 expression was required to deplete nucleosomes across a regulatory element located within the *Cd79a* locus (Fig. 3b; **right**).

The increase in accessibility observed in BLPs may simply reflect increased abundance of the B-lineage-specific transcription factors. To exclude this possibility, we examined E2A protein expression in ALPs and BLPs using E2A-GFP mice[32]. We found that E2A protein abundance did not change during the ALP to BLP transition (Fig. 3c). Likewise, E2A (*Tcf3*)

and Ikaros (*Ikzf1*) transcript abundance was equivalent in ALPs versus BLPs (Fig. 3d). Thus, the enhancement in open chromatin seen at E2A binding sites in Brg1-proficient BLPs compared to ALPs cannot readily be explained in terms of elevated protein expression. Rather, we suggest that Brg1 facilitates nucleosome depletion across an enhancer repertoire closely associated with a B-lineage specific program of gene expression.

Brg1 is essential to promote *Igh locus* contraction

Since Brg1 abundance is particularly high in pro-B cells and Brg1 binds collaboratively with factors that are associated with *Igh* locus contraction, we inspected the *Igh* locus for Brg1 occupancy. As previously reported, Brg1 bound to the J_H gene segments (Fig. 4a)[21]. Brg1 occupancy was not limited, however, to the J_H elements. Rather, Brg1 binding was dispersed throughout the *Igh* locus and overlapped with the deposition of H3K4me2 and nucleosome depleted regions as revealed by ATAC-Seq (Fig. 4a). Upon inspecting Hi-C data (meta-analysis) generated from pro-B cells, we observed an intricate pattern of significant short-range genomic interactions that span the entire V_H region cluster, consistent with an organization of bundles of loops (Fig. 4a)[33, 34]. Notably, we identified a giant loop connecting the extreme ends of the *Igh* locus, identifying the boundaries that define the *Igh* topological domain (Fig. 4a). We also identified a spectrum of long-range genomic interactions involving distal V_H region cluster and *Igh* gene segments across the 3′-end of the locus and found that a subset of these putative anchors was enriched for Brg1 occupancy (Fig. 4a,b). Genomic interactions involving Brg1 were primarily enriched for lineage-specific transcription factors, including Pax5, EBF1, YY1, Ikaros and E2A as well as Med1 (Fig. 4c).

To determine whether Brg1 modulated the accessibility of transcription factor binding sites across the *Igh* locus, Brg1-proficient and Brg1-deficient pro-B cells were inspected for ATAC-Seq reads. Pro-B cells were isolated from *Smarca4*$^{+/+}$ER-Cre and *Smarca4*$^{fl/fl}$ER-Cre BM B220^{+} cells and expanded in the presence of IL-7 and SCF. We found that the majority of pro-B cells were depleted for Brg1 protein upon culturing the cells for three days in the presence of tamoxifen (data not shown). As predicted, loss of Brg1 expression was closely associated with decreased chromatin accessibility for a large fraction of sites (50%) bound by lineage-specific transcription factors but not CTCF (Fig. 4d,e). RNA transcript abundance of lineage-specific transcription factors was not affected upon depletion of Brg1 expression (Supplementary Fig. 5a). Consistent with reduced Pax5 and YY1 binding, we observed a reduction in antisense transcription associated with distal regulatory regions, named PAIR elements (Supplementary Fig. 5c)[35, 36].

Our findings indicated that Brg1 occupancy across the *Igh* locus was closely associated with transcription factor binding sites. A number of these transcription factor-binding sites have previously been implicated in *Igh* locus contraction. These observations raised the possibility that Brg1 acts to evict nucleosomes positioned across regulatory elements that mediate long-range genomic interactions. To examine this possibility, we measured the spatial distances separating the distal V_H region cluster from a genomic region located 3′ of the *Igh* locus. Specifically, *Rag1*$^{-/-}$ pro-B cells were depleted for Brg1 expression using an shRNA directed against *Smarca4*. The *Igh* locus topology of the transduced pro-B cells was

then examined by 3D-FISH. Notably, we found that the *Igh* locus displayed significant long-range locus decontraction upon depletion of Brg1 expression in the pro-B cell population (Fig. 4f and Supplementary Fig. 5b). Since a reduced contraction should lead to preferred usage of the proximal V_H segments, we assessed proximal and distal V_H segments usage in pre-B cells sorted from *Smarca4*$^{fl/+}$*Il7r*$^{Cre/+}$ or *Smarca4*$^{fl/fl}$*Il7r*$^{Cre/+}$ mice. In agreement with the reduction in *Igh* locus contraction, we found a significant increase in the usage of proximal V_H7183 genes when compared to the distal J_H558 segments (Fig. 4g). Taken together, these observations indicate that the chromatin remodeler Brg1 is essential to promote *Igh* locus contraction.

Brg1 regulates *Myc* expression to promote pro-B cell growth

To determine whether in committed pro-B cells Brg1 acts to maintain an active enhancer repertoire, RNA was isolated from Brg1-proficient and Brg1-deficient pro-B cells and analyzed by RNA-Seq. We found that approximately 1800 genes displayed significant differences in transcript abundance in pro-B cells depleted for Brg1 expression as compared to Brg1-proficient pro-B cells (Fig. 5a). We found that at least 1000 genes showed two-fold changes or more in expression upon depletion of Brg1 (Supplementary Table 1). Notably, gene ontology analysis showed that the absence of Brg1 affected the expression of a spectrum of genes associated with ribosome biogenesis (Fig. 5b). Transcript abundance associated with the metabolism of rRNA and non-coding RNA (ncRNA) synthesis also declined in Brg1-deficient pro-B cells (Fig. 5b). Finally, we found that *Myc* transcript abundance declined significantly in Brg1-deficient pro-B cells (Fig. 5a). Real-time PCR confirmed the downregulation of *Myc* expression in Brg1-deficient pro-B cells and was also observed in *Rag1*$^{-/-}$ pro-B cells transduced with an shRNA directed against *Smarca4* (Fig. 5c).

The decline in *Myc* transcript abundance upon depletion of Brg1 expression raises the question as to how Brg1 regulates *Myc* expression. As a first approach to address this question we inspected the *Myc* locus for Brg1 occupancy. Brg1 occupancy was particularly prominent in a distally located regulatory element previously shown to modulate *Myc* expression in leukemic cells[37]. We found that in pro-B cells, the distally located super-enhancer showed deposition of H3K4me2 and was associated with Brg1, EBF1, Ikaros and Pax5 occupancy (Fig. 5d,e). Furthermore, Hi-C reads showed that in pro-B cells the super-enhancer contacted the *Myc* promoter with relatively high frequencies (Fig. 5d). To assess whether Brg1 expression is required to permit B-lineage specific transcription factors access to the *Myc* super-enhancer, we examined Ikaros occupancy using chromatin-immunoprecipitation in conjunction with Ikaros antibodies in wild-type and Brg1-deficient pro-B cells. Indeed, in the absence of Brg1, Ikaros occupancy at the *Myc* super-enhancer declined significantly (Fig. 5f). To directly assess whether Brg1 expression was required to evict nucleosomes across the *Myc* super-enhancer, Brg1-proficient and Brg1-deficient pro-B cells were analyzed for chromatin accessibility using ATAC sequencing. As expected, we found that Brg1 expression modulated chromatin accessibility to the *Myc* super-enhancer (Fig. 5e).

c-Myc is known to control cell growth by regulating ribosome biogenesis[38]. To determine whether c-Myc directly regulated the expression of genes that regulate ribosome biogenesis, we examined c-Myc occupancy in pro-B cells using ChIP-Seq data. Notably, we observed c-Myc binding in pro-B cells in promoter regions of genes associated with ribosome biogenesis, including *Tsr1 a*nd *Gar1* (Fig. 6a). These findings raised the possibility that in pro-B cells, Brg1 activates *Myc* expression, which in turn, acts to induce the expression of an ensemble of genes involved in ribosome biogenesis. We found that the expression of genes associated with c-Myc binding in pro-B cells declined significantly in Brg1-deficient when compared to Brg1-proficient pro-B cells (Fig. 6b). Globally, approximately 12% of the genes that showed decreased transcript abundance in *Smarca4*$^{\Delta/\Delta}$ pro-B cells as compared to *Smarca4*$^{+/+}$ pro-B cells were direct c-Myc targets (Supplementary Table 1).

To assess directly whether Brg1 acts to regulate pro-B cell growth, the expansion of wild-type pro-B cells and pro-B cells depleted for Brg1 expression in mice was monitored using BrdU labeling. Specifically, 4 h post injection with BrdU, the BMs derived from *Smarca4*$^{fl/+}$*Il7r*$^{Cre/+}$ and *Smarca4*$^{fl/fl}$*Il7r*$^{Cre/+}$ mice were isolated and analyzed for BrdU incorporation in the pro-B cell compartment. As predicted, BrdU incorporation in the pro-B population isolated from *Smarca4*$^{fl/fl}$*Il7r*$^{Cre/+}$ mice displayed a significantly reduced degree of proliferation when compared to control cells (Fig. 6c). Taken together, these observations indicate that, in pro-B cells, Brg1 permits a subset of B-lineage transcription factors access to a super-enhancer to directly activate *Myc* expression, which in turn induces the expression of genes associated with ribosome biogenesis, to control the growth of pro-B cells.

Brg1 enforces a pro-B cell specific transcription signature

To examine in greater detail the spectrum of genes affected by the loss of Brg1 expression, we compared the differences in transcript abundance of Brg1-proficient versus Brg1-deficient pro-B cells to the change during the CLP to pro-B cell transition. The transcription signatures of pro-B cells depleted for Brg1 expression as compared to wild-type pro-B cells did not correlate with changes in expression that occur during the CLP to pro-B cell transition (Fig. 7a, *left*). However, the transcription profiles of Brg1-deficient pro-B cells versus wild-type pro-B cells correlated with changes in transcription signatures that accompany the pro-B to the pre-B cell transition (Fig. 7a, *right*). For example, *Cd79b* transcripts were increased whereas *Dntt* abundance declined in the absence of Brg1 (data not shown). These data suggest that Brg1 acts in pro-B cells to suppress a pre-B lineage-specific pattern of gene expression. To validate these findings *in vivo* we examined *Smarca4*$^{fl/+}$*Il7r*$^{Cre/+}$ and *Smarca4*$^{fl/fl}$*Il7r*$^{Cre/+}$ mice for changes in the pro-B versus pre-B cell ratio. As predicted, we found that the ratio of small pre-B cells to pro-B cells was significantly altered in mice depleted for Brg1 expression (Fig. 7b). Notably, the large pre-B cell was severely affected in B cell progenitors, consistent with a requirement for Brg1 to promote cell growth (Supplementary Fig. 6a). In further support of this notion, sorted pro-B cells derived from *Smarca4*$^{fl/fl}$ER-Cre mice treated with tamoxifen led to a preferential loss of large cells and an increase in the fraction of small pre-B cells as compared to sorted *Smarca4*$^{+/+}$ER-Cre pro-B cells (Supplementary Fig. 6b,c). To determine how these findings mechanistically relate to changes in transcription signatures during the proB to pre-B cell transition, we assigned c-Myc binding sites to the nearest transcription start site and

compared c-Myc occupancy to gene expression patterns in pro-B versus pre-B cells. Notably, we found that the expression of an ensemble of genes associated with c-Myc bound sites in pro-B cells was closely associated with a pro-B developmental stage-specific program of gene expression (Fig. 7c). Taken together, these data indicate that the chromatin remodeler Brg1 acts to prevent premature differentiation of pro-B cells into the pre-B cells by regulating *Myc* expression.

DISCUSSION

It is now established that during developmental progression, transcriptional regulators act collaboratively to establish *de novo* enhancer repertoires as cells differentiate along distinct trajectories[39, 40]. The development of early B cell progenitors is among the best characterized in terms of transcription factors that modulate the developmental progression. However, it is less clear how lineage-specific transcription factors activate *de novo* or poised enhancer repertoires to initiate lineage-specific programs of gene expression. Previous studies have demonstrated that chromatin remodelers, including the BAF complex, act to promote nucleosome depletion to permit transcription factors access to their cognate binding sites[41, 42]. Here, we have mapped the spectrum of Brg1 binding sites across the pro-B cell genome. We found that Brg1 occupancy did not overlap with one distinct transcription factor but rather with combinations of transcription factors including E2A, EBF1, Ikaros and members of the IRF family. How, then, is Brg1 recruited to a B-lineage specific enhancer repertoire that harbors different and unique combinations of transcription factor binding sites? We found that in pro-B cells, Brg1 and p300 occupancy overlapped across the majority of the pro-B enhancer repertoire. p300 is recruited to active enhancer elements by directly interacting with a multitude of transcription factors[43]. Thus, we propose that in the CLP compartment, E2A, Foxo1, Ikaros and EBF1 bind to a primed and partially opened enhancer repertoire. This binding results in the recruitment of p300, a histone acetylase, to an ensemble of B-lineage specific enhancers. The sequestration of p300 to poised enhancers leads to the deposition of H3K27ac, which recruits Brg1, which in turn, evicts and/or slides nucleosomes away from the poised enhancer repertoire.

The role of Brg1 in B cell development is not restricted to the specification of the B cell fate. Our data point to multiple roles for Brg1 in committed B-lineage cells including *Igh* locus contraction. In developing B cell progenitors, the *Igh* locus undergoes large-scale alterations merging the proximal and distal V_H regions into a singular domain as progenitors differentiate into pro-B cells[12]. How does a chromatin remodeler like Brg1 promote the merging of chromatin domains? We found that Brg1 binds to multiple sites scattered across the entire *Igh* locus. Previous studies have demonstrated that *Igh* locus contraction is regulated by multiple transcription factors, including E2A, Pax5, Ikaros and YY1[13–15]. Here, we demonstrate that Brg1 expression is essential to evict nucleosomes across *Igh* locus regulatory elements containing clusters of Pax5, YY1, E2A and EBF1 binding sites. We find that a subset of these sites is associated with long-range genomic interactions that connect the distal V_H regions cluster with more proximally located anchors plausibly to promote *Igh* locus contraction.

Our data also indicate that Brg1 acts in committed pro-B cells to maintain *Myc* expression and promote cell growth. Brg1 is required to activate *Myc* expression by associating with a distally located super-enhancer. The *Myc* distal super-enhancer has been previously identified in AML where Brg1 is essential to maintain *Myc* expression and promote the development of leukemia[37, 44]. We show that Brg1 is critical to maintain accessibility of this super-enhancer and allow for transcription factor binding. Downregulation of *Myc* caused further downregulation of genes associated with the control of lymphocyte cell growth. Specifically, a wide spectrum of genes that are associated with ribosome biogenesis, including factors associated with nucleoli and members of the exosome complex were downregulated in the absence of Brg1 and exhibited c-Myc binding. Consistent with these findings, we found that the large pre-B cell population was substantially decreased in Brg1-deficient mice. Thus, we suggest that Brg1 expression promotes the expansion of pro-B and large pre-B cells by elevating c-Myc abundance. Increased c-Myc levels, in turn, associate with a repertoire of promoters of genes associated with cell growth and protein synthesis. During the transition from the pro-B to the small resting pre-B cell stage, Brg1 levels decline as well as c-Myc levels. Interestingly, we found that depletion of Brg1 expression in the pro-B cell compartment led to the aberrant activation of a pre-B lineage specific transcription signature. Since we show that c-Myc occupancy is associated with pro-B lineage specific transcriptional program, we suggest that premature exit from the cell cycle through c-Myc downregulation induces a pre-B developmental stage-specific program of gene expression consistent with previous observations that connect exit from the cell cycle with developmental progression[45].

METHODS

Mice

Smarca4$^{fl/fl}$, *Il7r*$^{Cre/+}$, *Rosa26*$^{YFP/+}$, ER-CRE and E2A-GFP mice were bred and housed in specific pathogen–free conditions in accordance with the Institutional Animal Care and Use Committee of University of California, San Diego.

Flow cytometry

BM cells were harvested from femur, tibia and crista iliac. Cells were Fc-blocked (CD16/CD32, 2.4G2) and stained with the following FITC-, PerCP-Cy5.5-, PE-, PE-Cy7-, PE-CF594-, APC-, APC-Cy7-, PacificBlue-, eFluor450-, BV421- or biotinylated monoclonal antibodies: Flt3 (A2F10), CD11b (M1/70), GR1 (RB6-8C5), Ter119 (Ter119), CD3e (145-2c11), CD11c (N418), LY6c (AL-21), NK1.1 (PK136), B220 (RA3-6B2), CD117 (2B8), CD19 (1D3), IL7R (A7R34), IgD (11-26c), IgM (11/41), CD25 (pc61.5), Ly6d (49-H4), CD4 (GK1.5), CD8 (53–6.7), CD45.1 (A20), CD45.2 (104), CD115 (AFS98), pan-NK (DX5), followed by streptavidin-conjugated QD655 (Life Technologies) and propidium iodide. Antibodies were purchased from eBioscience with the exception of CD19 PE-CF594 (BD Biosciences), CD117 BV421 (BD Biosciences), B220 APCCy7 (BioLegend), CD19 APCCy7 (BioLegend) and Ly6D FITC (BD Biosciences). For sorting, BM cells were lineage-depleted before antibody staining with a cocktail of biotinylated antibodies (B220, Ter119, CD19, CD3, GR1, CD11c, CD11b, Ly6c, NK1.1 for CLP sorting and GR1, CD11b, Ter119 for pre-B cells sorting) followed by depletion using anti-biotin magnetic beads

(Miltenyi Biotech) on an autoMACS Separator. For BrdU incorporation, mice were injected i.p. with 200 μl BrdU labeling reagent (Life Technologies) 4 h before being sacrificed. BrdU staining was performed using the BrdU Staining Buffer Set for Flow Cytometry from eBioscience. DNase I (Sigma-Aldrich) treatment was performed for 1 h before incubation with anti-BrdU-FITC (eBioscience). Analysis was performed using an LSRII and cell sorting was performed on FACSAria II (BD Biosciences).

Cell culture and plasmids

Rag1-deficient pro-B cells were cultured in OPTI-MEM in presence of 10% FSC, 2x Penicillin-Streptomycin-Glutamine (PSG), 50 μM beta-mercaptoethanol (β-ME) and IL-7 and SCF homemade cytokines. The GFP cassette from pRVGP and pRVGP-BB was replaced with hCD25 cassette to generate *Ctrl*-sh and *Smarca4*-sh. Retroviral supernatant was obtained through 293T transfection by the calcium phosphate method with *Ctrl*-sh and *Smarca4*-sh in conjunction with the packaging plasmid pCL-Eco. Two days post-infection, infected cells were enriched with hCD25 magnetic beads (Miltenyi biotech) on an autoMACS separator. *Smarca4*$^{+/+}$ER-Cre and *Smarca4*$^{fl/fl}$ER-Cre pro-B cells were cultured as the Rag1-deficient pro-B cells. The Cre recombinase was activated by adding 4-OHT tamoxifen (Sigma-Aldrich) at 0.33 μM to the medium.

RT-PCR

Total RNA was isolated using RNeasy Mini Kit (Qiagen) or RNeasy Micro Kit (Qiagen). cDNA was generated with the First-strand synthesis kit (Life Technologies) using random hexamers. Quantitative PCR was performed using SYBR Green Master Mix (Roche) on Mx3500P cycler (Agilent Technologies). Primers were as follow:

Actb: 5′-GAAGCACTTGCGGTGCACGAT-3′ and 5′-TCCTGTGGCATCCATGAAACT-3′,

Brg1: 5′-CACCTAACCTCACCAAGAAGATGA-3′ and 5′-CTTCTTGAAGTCCACAGGCTTTC-3′,

Brm: 5′-AGGACGTGGACGACGAATAC-3′ and 5′-AATGGTCTGGATGGTCTTGC-3′,

Myc: 5′-CCTAGTGCTGCATGAGGAGAC-3′ and 5′-CCTCATCTTCTTGCTCTTCTTCA-3′,

Tcf3: 5′-GGGAGGAGAAAGAGGATGA-3′ and 5′-CCGGTCCCTCAGGTCCTTC-3′,

Ebf1: 5′-GCCTTCTAACCTGCGGAAATCCAA-3′ and 5′-GGAGCTGGAGCCGGTAGTGGAT-3′,

Ikzf1: 5′-GGAGGCACAAGTCTGTTGAT-3′ and 5′-CATTTCACAGGCACGCCCATTCT-3′.

RNA-Seq

Total RNA was isolated using RNeasy Mini kit (Qiagen). RNA was treated with TURBO DNase (Life Technologies). mRNA was purified from total RNA using Dynabeads mRNA

purification kit (Life Technologies). cDNA was generated with the First-strand synthesis kit (Life Technologies) using a combination of random hexamers and oligo(dT) in presence of actinomycin D. Second-strand synthesis was performed with dUTP instead of dTTP. The ds-cDNA was sonicated to 200–400 bp using the S220 Focused-ultrasonicator (Covaris). Sonicated cDNA was ligated to adaptors (NEBNext primer kit). The resulting DNA was treated with uracil-N-glycolsylase prior to PCR amplification with the indexing primers (NEBNext primer kit). Following PCR, fragments were size-selected. To perform RNA-Seq analysis, we sequenced at a depth of 10–15M reads per sample using an Illumina Hiseq2500. Raw sequencing files were quality controlled with FastQC (http://www.bioinformatics.babraham.ac.uk/projects/fastqc/). Alignment and trimming of reads was performed using the OSA algorithm against the mm10 mouse genome reference in Arraystudio (Omicsoft, http://bioinformatics.oxfordjournals.org/content/early/2012/05/15/bioinformatics.bts294). RNA transcripts were quantified using RSEM methods as implemented in Arraystudio (http://deweylab.biostat.wisc.edu/rsem/; Omicsoft). Principal Component Analysis (PCA) was then performed to check for possible batch effects and outliers. Abundance values (counts) were normalized and compared between samples using DESeq (http://www-huber.embl.de/users/anders/DESeq/).

ATAC-Seq

ATAC-Seq was performed as described[31]. Briefly, cells were lysed. Nuclei were tagmented for 30min at 37 °C with the Nextera DNA Sample Preparation Kit. Tagmented DNA was cleaned up using DNA Clean and Concentrator columns (ZymoResearch). Library fragments were amplified using 1x NEB next PCR master mix and custom Nextera PCR primers 1–6. Number of cycles was determined by qPCR as described. Libraries were purified on DNA Clean and Concentrator columns. Libraries were sequenced on HiSeq 2500 as single reads. Reads were aligned to mm9 using Bowtie with the parameter –m 1 (http://bowtie-bio.sourceforge.net). Data was analyzed using HOMER (http://homer.salk.edu/homer). Tag directories were generated using parameter – tbp 1, which removed most of the reads arising from mitochondrial DNA.

ChIP and ChIP-Seq

Cells were fixed for 15 min in PBS 1.5mM ethylene glycol-bis(succinic acid N-hydroxysuccinimideester) (EGS), followed by 15 min with 1% formaldehyde. Formaldehyde was quenched for 10 min with 0.2 M glycine. Cells were washed 2 times with PBS and pellets were frozen in liquid nitrogen. 30 μl Protein G Dynabeads (Life Technologies) were blocked with 0.5% BSA (w/v) in PBS. Magnetic beads were bound with 6 μg of indicated antibody. Antibodies used were as follow: Brg1: Millipore 07-478 and Ikaros: Ik-C was a kind gift from S. Smale. Cross-linked cells were lysed in lysis buffer 1 (50 mM HEPES pH7.5, 140 mM NaCl, 1 mM EDTA, 10% glycerol, 0.5% NP-40, 0.25% TritonX-100) and washed with lysis buffer 2 (10 mM Tris-HCl pH8.0, 200 mM NaCl, 1 mM EDTA, 0.5 mM EGTA). Cells were resuspended and sonicated in lysis buffer 3 (10 mM Tris-HCl pH8.0, 100 mM NaCl, 1 mM EDTA, 0.5 mM EGTA, 0.1% Na-Deoxycholate, 0.5% N-lauroylsarcosine) for 10 cycles at 10 sec each on ice (20W) with 50 s on ice between cycles. Lysates were cleared by centrifugation and Triton X-100 was added at a final concentration of 1%. Lysates were then incubated overnight at 4 °C with the previously

prepared magnetic beads. Beads were washed once with RIPA (50 mM Tris-HCl pH8.0, 150 mM NaCl, 0.1% SDS, 0.1% Na-Deoxycholate, 1% Triton X-100, 1 mM EDTA), once with RIPA 500 (50 mM Tris-HCl pH8.0, 500 mM NaCl, 0.1% SDS, 0.1% Na-Deoxycholate, 1% Triton X-100, 1 mM EDTA), once with LiCl wash (10 mM Tris-HCl pH8.0, 250 mM LiCl, 0.5% NP-40, 0.5% Na-deoxycholate, 1 mM EDTA) and finally twice with TE (10 mM Tris pH8.0, 1mM EDTA). Bound complexes were eluted from the beads in elution buffer (10 mM Tris-HCl pH8.0, 0.5% SDS, 300 mM NaCl, 5 mM EDTA) for 30 min at 65 °C with shaking. Crosslinks were reversed overnight at 65 °C. RNA and protein were digested in the supernatant using RNase A and Proteinase K and DNA was purified using ChIP DNA clean and concentrator columns (Zymoresearch).

Libraries were prepared with the NEBNext primer set and were size-selected on an 8% PAGE gel. Libraries were run on Illumina HiSeq 2500. Reads were aligned to mm9 using Bowtie with the parameter –m 1 (http://bowtie-bio.sourceforge.net). Data was analyzed using HOMER (http://homer.salk.edu/homer). For Ikaros ChIP, ChIP primers were as follow: Site1: 5′-CCTGGTTCCGAGAAGTCACT-3′ and 5′-GCACTCTCTGGAAAGGGTCT-3′, Site2: 5′-TCTCCTAGCCCCTAAGACCA-3′ and 5′-GGAGTTGCCCTTGGAGATCC-3′.

Hi-C analysis

Reads were aligned to mm9 using Bowtie with the parameter –m 1 (http://bowtie-bio.sourceforge.net). Data was analyzed using HOMER (http://homer.salk.edu/homer). Interactions were depicted using circos (http://circos.ca/). The results for all pair-wise comparisons between the different features at the interactions end-points were visualized using cytoscape (http://www.cytoscape.org/).

Imaging

Fluorescent *in situ* hybridization was performed as described previously[12]. The bacterial artificial chromosomes (BAC) probes used were RP23-201H14 and RP24-189H12 from the BACPAC Resource Center at Children's Hospital Oakland Research Institute. Three-dimensional fluorescent images were acquired on a deconvolution microscope (Deltavision). Optical sections (*z*-stacks), 0.2 μm apart, were obtained throughout the cell volume in the appropriate channels. Distances between the BAC probes were obtained with the softWoRx program by calculating the distances between the centers of mass of the probes. Probe RP23-201H14 was labeled with Alexa Fluor 568-5-dUTP and probe RP24-189H12 was labeled with Alexa Fluor 488-5-dUTP.

PCRs for Igh recombination

Genomic DNA was purified from sorted pre-B cells PCR on DNeasy Mini Columns (Qiagen). PCR reactions were performed on 25, 6.75 and 1.2 ng of genomic DNA using forward primers V_H7183: 5′-GAASAMCCTGTWCCTGCAAATGASC-3′ and V_HJ558: 5′-CARCACAGCCTWCATGCARCTCARC-3′ and reverse primer J_H3: 5′-CTCACAAGAGTCCGATAGACCCTGG-3′. PCR products were electrophoresed on 1.5% agarose gel, blotted on nylon membrane and hybridized with radioactive probe. Signals were

detected with a Phosphorimager (GE Healthcase) and analyzed with the ImageJ software (http://imagej.nih.gov/ij).

Publically available datasets

PU.1: GSE21512, CTCF, c-Myc, p300 and H3K4me2: GSE40173, E2A, H3K4me1 and H3K4me3: GSE21978, EBF: GSE53595, Pax5: GSE38046, YY1: GSE43008, Med1: GSE44288, Hi-C: GSE35519 and GSE40173.

Statistical methods

Data were analyzed with a two-tailed Student *t* test for two groups comparison. *P* values of less than 0.05 were considered statistically significant. No blinding was performed for the animal studies and no animal was excluded from the analysis. For FISH experiments, the investigator measuring the distance between the probes was unaware of the sample. The distance between the probes was only measured in cells where the probes could be detected for both alleles.

Supplementary Material

Refer to Web version on PubMed Central for supplementary material.

Acknowledgments

We thank L. Edsall, S. Kuan, B. Li, B. Ren for sequencing. ATAC-sequencing was partly conducted at the IGM Genomics Center, University of California, San Diego, La Jolla, CA, supported by grant # P30CA023100. Imaging was performed at the microscopy core of the School of Medicine, University of California, San Diego, La Jolla, CA, supported by grant #NS047101. We thank the Murre laboratory for helpful discussions and in particular A. Bortnick for comments on the manuscript. We thank B. Bruneau (Gladstone Institute of Cardiovascular Disease, San Francisco, USA) and P. Chambon (IGBMC, Strasbourg, France) for *Smarca4*$^{fl/fl}$ mice, Y. Zhuang (Duke University, Durham, USA) for E2A-GFP mice, S.Smale (UCLA, Los Angeles, USA) for pRVGP and pRVGP-BB plasmids and Ik-C antibody. H.R.R. was supported by DFG-SFB 873-project B11. C.B. was partly supported by the European Molecular Biology Organization as well as by the Swiss National Science Foundation. This work was supported by the NIH RO1 AI109599-25 (C.M.).

References

1. DeKoter RP, Kamath MB, Houston IB. Analysis of concentration-dependent functions of PU.1 in hematopoiesis using mouse models. Blood Cells Mol Dis. 2007; 39:316–320. [PubMed: 17629523]
2. Wang JH, et al. Selective defects in the development of the fetal and adult lymphoid system in mice with an Ikaros null mutation. Immunity. 1996; 5:537–549. [PubMed: 8986714]
3. Inlay MA, et al. Ly6d marks the earliest stage of B-cell specification and identifies the branchpoint between B-cell and T-cell development. Genes Dev. 2009; 23:2376–2381. [PubMed: 19833765]
4. Mansson R, et al. B-lineage commitment prior to surface expression of B220 and CD19 on hematopoietic progenitor cells. Blood. 2008; 112:1048–1055. [PubMed: 18495958]
5. Mansson R, et al. Positive intergenic feedback circuitry, involving EBF1 and FOXO1, orchestrates B-cell fate. Proc Natl Acad Sci U S A. 2012; 109:21028–21033. [PubMed: 23213261]
6. Langdon WY, Harris AW, Cory S, Adams JM. The c-myc oncogene perturbs B lymphocyte development in E-mu-myc transgenic mice. Cell. 1986; 47:11–18. [PubMed: 3093082]
7. Vallespinos M, et al. B Lymphocyte commitment program is driven by the proto-oncogene c-Myc. J Immunol. 2011; 186:6726–6736. [PubMed: 21572027]
8. Heizmann B, Kastner P, Chan S. Ikaros is absolutely required for pre-B cell differentiation by attenuating IL-7 signals. J Exp Med. 2013; 210:2823–2832. [PubMed: 24297995]

9. Joshi I, et al. Loss of Ikaros DNA-binding function confers integrin-dependent survival on pre-B cells and progression to acute lymphoblastic leukemia. Nat Immunol. 2014; 15:294–304. [PubMed: 24509510]
10. Schwickert TA, et al. Stage-specific control of early B cell development by the transcription factor Ikaros. Nat Immunol. 2014; 15:283–293. [PubMed: 24509509]
11. Johnston CM, Wood AL, Bolland DJ, Corcoran AE. Complete sequence assembly and characterization of the C57BL/6 mouse Ig heavy chain V region. J Immunol. 2006; 176:4221–4234. [PubMed: 16547259]
12. Jhunjhunwala S, et al. The 3D structure of the immunoglobulin heavy-chain locus: implications for long-range genomic interactions. Cell. 2008; 133:265–279. [PubMed: 18423198]
13. Seet CS, Brumbaugh RL, Kee BL. Early B cell factor promotes B lymphopoiesis with reduced interleukin 7 responsiveness in the absence of E2A. J Exp Med. 2004; 199:1689–1700. [PubMed: 15210745]
14. Liu H, et al. Yin Yang 1 is a critical regulator of B-cell development. Genes Dev. 2007; 21:1179–1189. [PubMed: 17504937]
15. Fuxa M, et al. Pax5 induces V-to-DJ rearrangements and locus contraction of the immunoglobulin heavy-chain gene. Genes Dev. 2004; 18:411–422. [PubMed: 15004008]
16. Calo E, Wysocka J. Modification of enhancer chromatin: what, how, and why? Mol Cell. 2013; 49:825–837. [PubMed: 23473601]
17. Creyghton MP, et al. Histone H3K27ac separates active from poised enhancers and predicts developmental state. Proc Natl Acad Sci U S A. 2010; 107:21931–21936. [PubMed: 21106759]
18. Kagey MH, et al. Mediator and cohesin connect gene expression and chromatin architecture. Nature. 2010; 467:430–435. [PubMed: 20720539]
19. Whyte WA, et al. Master transcription factors and mediator establish super-enhancers at key cell identity genes. Cell. 2013; 153:307–319. [PubMed: 23582322]
20. Ho L, Crabtree GR. Chromatin remodelling during development. Nature. 2010; 463:474–484. [PubMed: 20110991]
21. Morshead KB, Ciccone DN, Taverna SD, Allis CD, Oettinger MA. Antigen receptor loci poised for V(D)J rearrangement are broadly associated with BRG1 and flanked by peaks of histone H3 dimethylated at lysine 4. Proc Natl Acad Sci U S A. 2003; 100:11577–11582. [PubMed: 14500909]
22. Osipovich OA, Subrahmanyam R, Pierce S, Sen R, Oltz EM. Cutting edge: SWI/SNF mediates antisense Igh transcription and locus-wide accessibility in B cell precursors. J Immunol. 2009; 183:1509–1513. [PubMed: 19596997]
23. Gao H, et al. Opposing effects of SWI/SNF and Mi-2/NuRD chromatin remodeling complexes on epigenetic reprogramming by EBF and Pax5. Proc Natl Acad Sci U S A. 2009; 106:11258–11263. [PubMed: 19549820]
24. Choi J, et al. The SWI/SNF-like BAF complex is essential for early B cell development. J Immunol. 2012; 188:3791–3803. [PubMed: 22427636]
25. Indra AK, et al. Temporally controlled targeted somatic mutagenesis in embryonic surface ectoderm and fetal epidermal keratinocytes unveils two distinct developmental functions of BRG1 in limb morphogenesis and skin barrier formation. Development. 2005; 132:4533–4544. [PubMed: 16192310]
26. Schlenner SM, et al. Fate mapping reveals separate origins of T cells and myeloid lineages in the thymus. Immunity. 2010; 32:426–436. [PubMed: 20303297]
27. Kim J, et al. Ikaros DNA-binding proteins direct formation of chromatin remodeling complexes in lymphocytes. Immunity. 1999; 10:345–355. [PubMed: 10204490]
28. O'Neill DW, et al. An ikaros-containing chromatin-remodeling complex in adult-type erythroid cells. Mol Cell Biol. 2000; 20:7572–7582. [PubMed: 11003653]
29. Ikawa T, Kawamoto H, Wright LY, Murre C. Long-term cultured E2A-deficient hematopoietic progenitor cells are pluripotent. Immunity. 2004; 20:349–360. [PubMed: 15030778]
30. Lin YC, et al. A global network of transcription factors, involving E2A, EBF1 and Foxo1, that orchestrates B cell fate. Nat Immunol. 2010; 11:635–643. [PubMed: 20543837]

31. Buenrostro JD, Giresi PG, Zaba LC, Chang HY, Greenleaf WJ. Transposition of native chromatin for fast and sensitive epigenomic profiling of open chromatin, DNA-binding proteins and nucleosome position. Nat Methods. 2013; 10:1213–1218. [PubMed: 24097267]
32. Zhuang Y, Jackson A, Pan L, Shen K, Dai M. Regulation of E2A gene expression in B-lymphocyte development. Mol Immunol. 2004; 40:1165–1177. [PubMed: 15104122]
33. Zhang Y, et al. Spatial organization of the mouse genome and its role in recurrent chromosomal translocations. Cell. 2012; 148:908–921. [PubMed: 22341456]
34. Lin YC, et al. Global changes in the nuclear positioning of genes and intra- and interdomain genomic interactions that orchestrate B cell fate. Nat Immunol. 2012; 13:1196–1204. [PubMed: 23064439]
35. Ebert A, et al. The distal V(H) gene cluster of the Igh locus contains distinct regulatory elements with Pax5 transcription factor-dependent activity in pro-B cells. Immunity. 2011; 34:175–187. [PubMed: 21349430]
36. Medvedovic J, et al. Flexible long-range loops in the VH gene region of the Igh locus facilitate the generation of a diverse antibody repertoire. Immunity. 2013; 39:229–244. [PubMed: 23973221]
37. Shi J, et al. Role of SWI/SNF in acute leukemia maintenance and enhancer-mediated Myc regulation. Genes Dev. 2013; 27:2648–2662. [PubMed: 24285714]
38. van Riggelen J, Yetil A, Felsher DW. MYC as a regulator of ribosome biogenesis and protein synthesis. Nat Rev Cancer. 2010; 10:301–309. [PubMed: 20332779]
39. Heinz S, et al. Simple combinations of lineage-determining transcription factors prime cis-regulatory elements required for macrophage and B cell identities. Mol Cell. 2010; 38:576–589. [PubMed: 20513432]
40. Lara-Astiaso D, et al. Chromatin state dynamics during blood formation. Science. 2014; 345:943–949. [PubMed: 25103404]
41. Fan HY, He X, Kingston RE, Narlikar GJ. Distinct strategies to make nucleosomal DNA accessible. Mol Cell. 2003; 11:1311–1322. [PubMed: 12769854]
42. Ramirez-Carrozzi VR, et al. Selective and antagonistic functions of SWI/SNF and Mi-2beta nucleosome remodeling complexes during an inflammatory response. Genes Dev. 2006; 20:282–296. [PubMed: 16452502]
43. Sakamoto S, et al. E2A and CBP/p300 act in synergy to promote chromatin accessibility of the immunoglobulin kappa locus. J Immunol. 2012; 188:5547–5560. [PubMed: 22544934]
44. Buscarlet M, et al. Essential role of BRG, the ATPase subunit of BAF chromatin remodeling complexes, in leukemia maintenance. Blood. 2014; 123:1720–1728. [PubMed: 24478402]
45. Clark MR, Mandal M, Ochiai K, Singh H. Orchestrating B cell lymphopoiesis through interplay of IL-7 receptor and pre-B cell receptor signalling. Nat Rev Immunol. 2014; 14:69–80. [PubMed: 24378843]

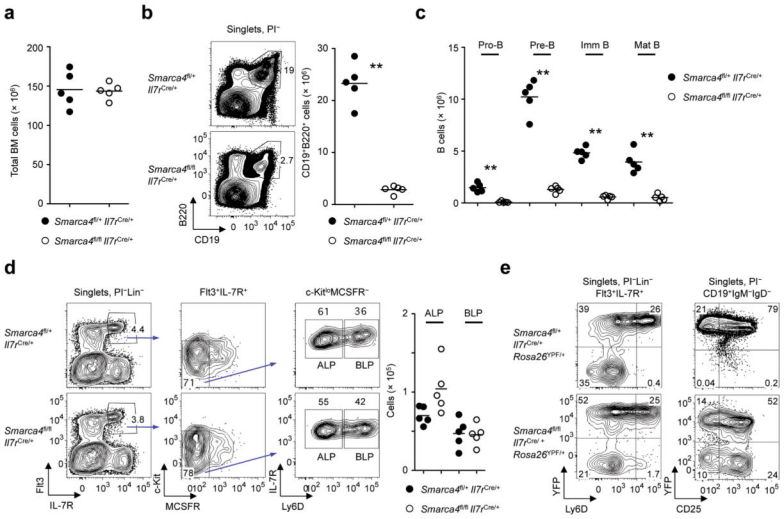

Figure 1.

The chromatin remodeler Brg1 is essential to specify B cell fate. (**a**) Normal bone marrow (BM) cellularity in *Smarca4*$^{fl/+}$*Il7r*$^{Cre/+}$ and *Smarca4*$^{fl/fl}$*Il7r*$^{Cre/+}$ mice. BM cells were derived from two femurs, two tibias and crista iliac. (**b**) B cell development is blocked in *Smarca4*$^{fl/fl}$*Il7r*$^{Cre/+}$ mice. BM cells were isolated from *Smarca4*$^{fl/+}$*Il7r*$^{Cre/+}$ and *Smarca4*$^{fl/fl}$*Il7r*$^{Cre/+}$ mice. Cells were gated as CD19^{+}B220^{+}. Percentages (left panel) as well as cellularity (right panel) are indicated. (**c**) Depletion of B cell progenitors in Brg1-deficient mice. BM cells were gated on the Gr1^{-}CD11b^{-}Ter119^{-}CD19^{+}B220^{+} population and segregated into pro-B (IgM^{-}IgD^{-}Kit^{+}CD25^{-}), pre-B (IgM^{-}IgD^{-}Kit^{-}CD25^{+}), immature B (imm B)(IgM^{+}IgD^{-}) and mature B (mat B) (IgM^{+}IgD^{+}) cells. Cell numbers are indicated for *Smarca4*$^{fl/+}$*Il7r*$^{Cre/+}$ and *Smarca4*$^{fl/fl}$*Il7r*$^{Cre/+}$ mice. (**d**) Normal numbers of CLPs in *Smarca4*$^{fl/fl}$*Il7r*$^{Cre/+}$ mice as compared to *Smarca4*$^{fl/+}$*Il7r*$^{Cre/+}$ mice. Left panels show the gating strategy to identify ALPs (Lin^{-}IL7R^{+}Flt3^{+}MCSFR^{-}Kit^{lo}Ly6D^{-}) and BLPs (Lin^{-}IL7R^{+}Flt3^{+}MCSFR^{-}Kit^{lo}Ly6D^{+}). Right panel indicates absolute numbers of ALPs and BLPs. (**e**) Cre recombinase activity in ALPs (Lin^{-}IL7R^{+}Flt3^{+}Ly6D^{-}) and BLPs (Lin^{-}IL7R^{+}Flt3^{+}Ly6D^{+}) (left panel) and proB and pre-B cells (as defined in **c**) (right panel) derived from *Smarca4*$^{fl/+}$*Il7r*$^{Cre/+}$*Rosa26*$^{YFP/+}$ and *Smarca4*$^{fl/fl}$*Il7r*$^{Cre/+}$*Rosa26*$^{YFP/+}$ mice. Left panel shows cells gated on Lin^{-}Flt3^{+}IL7R^{+}. Right panel shows cells gated on CD19^{+}B220^{+}IgM^{-}IgD^{-}. **a,b**: Representative of 4 independent experiments. **c–e**: Representative of 3 independent experiments. $^{**}P < 0.01$ (two-tailed unpaired Student's *t* test).

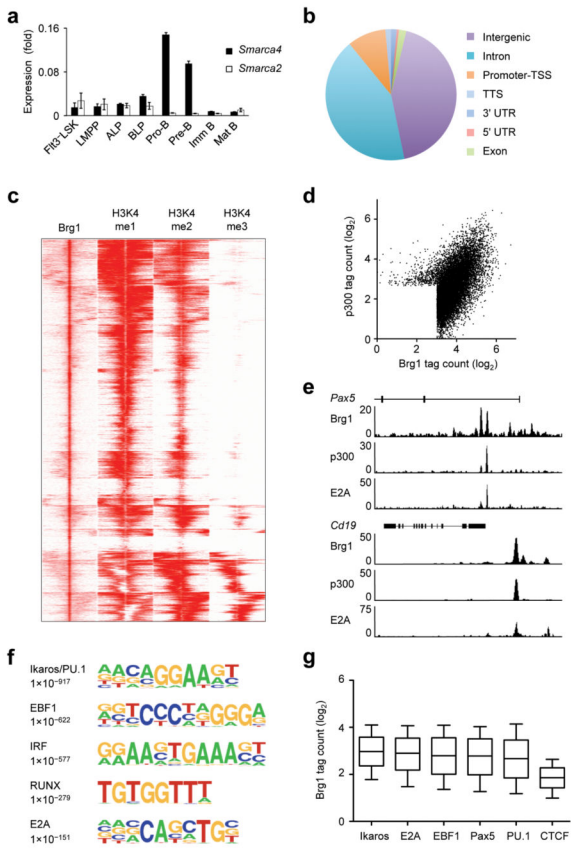

Figure 2.

Genome-wide Brg1 occupancy across the pro-B cell genome. (**a**) *Smarca4* and *Smarca2* transcript expression as fold relative to *Actb* during hematopoiesis and early B cell development. Error bars represent standard deviation from two independent sorts. (**b**) Distribution of 13169 Brg1 binding sites across genomic regions in *Rag1*$^{-/-}$ pro-B cells. (**c**) Heatmap of ChIP-Seq data gated on genome-wide Brg1-bound sites. The distribution of H3K4me1, H3K4me2 and H3K4me3 deposition in a 6-kb window across Brg1-bound sites is shown in *Rag1*$^{-/-}$ pro-B cells. (**d**) Brg1 and p300 tag count shown in a 200-bp window of Brg1 and p300 combined binding sites in *Rag1*$^{-/-}$ pro-B cells. (**e**) Brg1, p300 and E2A occupancy across *Pax5* (chr4: 44,703,000–44,730,000 in the mm9 build) and *Cd19* (chr7: 133,551,000–133,564,000) loci in *Rag1*$^{-/-}$ pro-B cells. (**f**) Cis-regulatory sequences associated with Brg1 occupancy. *P* values reflecting the significance of motif occurrence are shown. (**g**) Brg1 reads are shown for a 100-bp window centered on respectively 5000 Ikaros, E2A, EBF1, Pax5, PU.1 and CTCF binding sites.

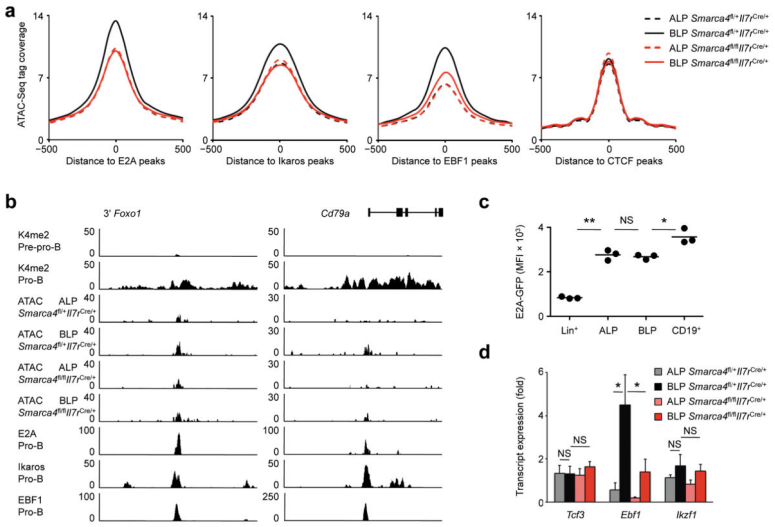

Figure 3.

Brg1 is required to establish an accessible B-lineage specific enhancer repertoire. (**a**) ATAC-Seq tag coverage in ALPs and BLPs derived from *Smarca4*$^{fl/+}$*Il7r*$^{Cre/+}$ and *Smarca4*$^{fl/fl}$*Il7r*$^{Cre/+}$ mice. ATAC reads are plotted as a function of genomic distance from E2A, Ikaros, EBF1 or CTCF bound-sites (identified in pro-B cells). (**b**) ATAC reads as well as deposition of H3K4me2, E2A, Ikaros and EBF1 occupancy are shown across the intergenic genomic regions flanking the *Foxo1* and *Cd79a* loci. Left panel indicates the genomic location of a 3′ *Foxo1* enhancer (chr3: 52,243,000 - 52,253,000). Right panel indicates the genomic location of a *Cd79a* regulatory region (chr7: 25,677,000 - 25,687,000). Pre-pro-B cells were represented by E2A-deficient multipotent progenitors. Pro-B cells were derived from *Rag1*$^{-/-}$ mice. (**c**) E2A-GFP mice were used to determine E2A protein abundance. Mean fluorescence intensity was determined in BM lineage^{+} cells (CD11b^{+}Ter119^{+}CD3^{+}NK1.1^{+}GR1^{+}), ALPs, BLPs and BM B cells (CD19^{+}). (**d**) Transcript expression was determined by RT-PCR in ALPs and BLPs sorted as in **a**. Fold relative to *Actb* expression. Average and error bars derived from triplicates. **a,b**: Data derived from two independent experiments. **c,d**: $^{**}P < 0.01$, $^{*}P < 0.05$ (two-tailed unpaired Student's *t* test)

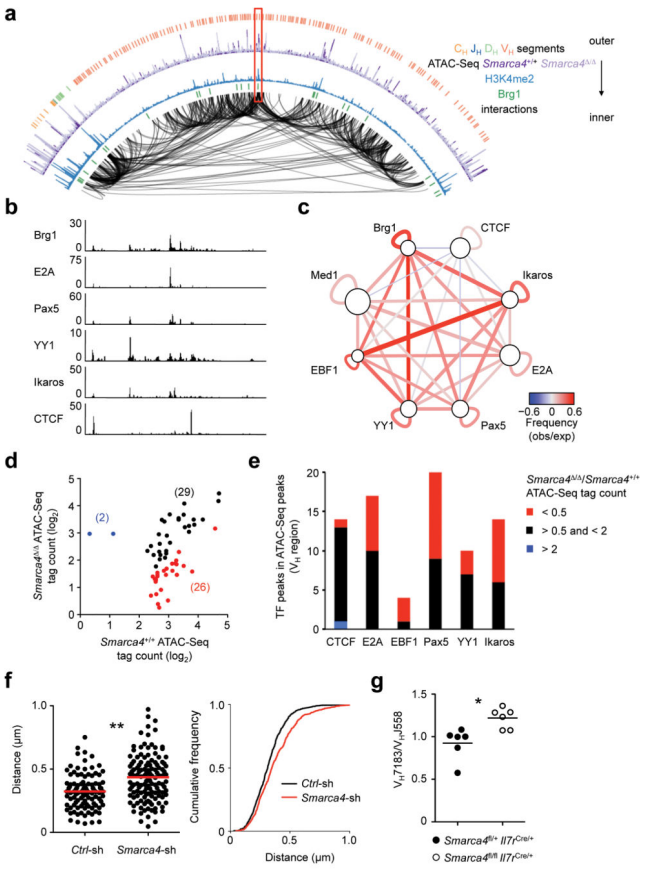

Figure 4.

Brg1 is essential to promote *Igh* locus contraction. (**a**) A meta-analysis for the pro-B cell interactome that were derived from Hi-C studies depicted as a Circos diagram (chr12: 114,300,000 - 117,400,000)[33,34]. Deposition of H3K4me2, region of open chromatin as determined by ATAC-Seq as well as Brg1 bound-sites are indicated. The thicknesses of the connecting lines reflect the natural log ratio of observed versus expected interaction frequency in the Hi-C data sets. Bin size used for the analysis was 10 kb. Constant, joining, diversity and variable regions are represented by different colors. (**b**) Brg1, E2A, Pax5, YY1, Ikaros and CTCF occupancy across the end point of interactions associated with the *Igh* locus (chr12: 115,825,000–115,875,00). (**c**) Relative frequencies by which lineage-specific transcription factors, CTCF and Med1 are associated with loop-attachment points (node size) and the significance and reproducibility of tethering, in terms of *P* values (line thickness). Color (red-blue) represents the log ratio of observed frequency relative to expected frequency (association strength). (**d**) ATAC-Seq tag count associated with *Smarca4*$^{+/+}$ and *Smarca4*$^{\Delta/\Delta}$ pro-B cells shown in combined ATAC-Seq peaks (57 peaks total) associated with the V_H region cluster. Regions of open chromatin with a 2-fold reduction and 2-fold increase in tag count in *Smarca4*$^{\Delta/\Delta}$ compared to *Smarca4*$^{+/+}$ pro-B cells are shown respectively in red and blue. Numbers of peaks are indicated in parenthesis. (**e**) Number of transcription factor peaks in region of open chromatin from **d** determined by ATAC-Seq in *Smarca4*$^{+/+}$ and *Smarca4*$^{\Delta/\Delta}$ pro-B cells. Transcription factor peaks associated with regions of open chromatin with a 2-fold reduction or 2-fold increase in tag

counts associated with *Smarca4*$^{\Delta/\Delta}$ pro-B cells as compared to *Smarca4*$^{+/+}$ pro-B cells are shown in red and blue, respectively. (**f**) The distribution of spatial distances separating the two BAC probes are shown for *Rag1*$^{-/-}$ cells transduced with control retrovirus or virus expressing an shRNA directed against *Smarca4*. Representative experiment of 5 independent experiments is shown. Right panel indicates the cumulative frequency distribution of the spatial distances that separate both BAC probes in control and Brg1-deficient pro-B cells. Data is derived from 5 independent experiments. (**g**) Decreased usage of distal V_H as compared to proximal V_H regions in Brg1-deficient pre-B cells. Usage of proximal V_H7183 segments compared to distal V_HJ558 segments was assessed by Southern blot in pre-B cells sorted from *Smarca4*$^{fl/+}$*Il7r*$^{Cre/+}$ and *Smarca4*$^{fl/fl}$*Il7r*$^{Cre/+}$ mice. Data is derived from two independent experiments. $^{**}P < 0.01$, $^{*}P < 0.05$ (two-tailed unpaired Student's *t* test).

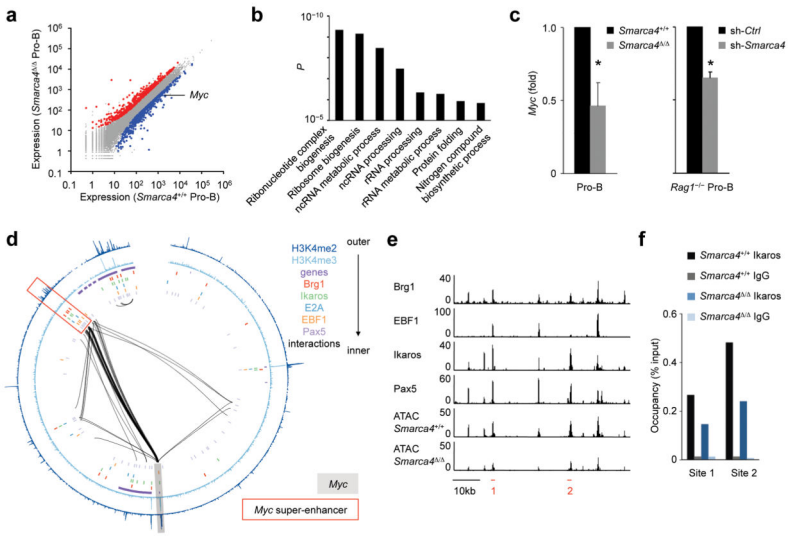

Figure 5.

Brg1 acts to induce the expression of *Myc* and an ensemble of genes associated with protein synthesis to regulate B cell growth. (**a**) RNA-Seq analysis of *Smarca4*$^{+/+}$ and *Smarca4*$^{\Delta/\Delta}$ pro-B cells. Expression represented as mean normalized counts. Abundance of transcripts significantly decreased (>two fold) in Brg1-deficient as compared to wild-type pro-B cells are highlighted in blue. Red dots indicate transcript levels that were significantly elevated (>two fold) in Brg1-ablated pro-B cells. (**b**) Brg1 regulates the expression of genes associated with protein synthesis at the pro-B cell stage. Ontology analysis (DAVID) shows clusters of genes that displayed decreased transcript abundance in *Smarca4*$^{\Delta/\Delta}$ pro-B cells compared to *Smarca4*$^{+/+}$ pro-B cells. (**c**) Brg1 regulates *Myc* expression in pro-B cells. RNA was isolated from wild-type or Brg1-depleted pro-B cells and analyzed by qPCR. Left panel shows *Myc* abundance in *Smarca4*$^{\Delta/\Delta}$ pro-B versus *Smarca4*$^{+/+}$ pro-B cells. Right panel shows *Myc* expression in *Rag1*$^{-/-}$ pro-B cells transduced with retrovirus expressing shRNAs directed against *Smarca4* versus transduced pro-B cells expressing a control vector. Fold relative to *Actb* expression. (**d**) Circos diagram depicting long-range genomic interactions (> 100 kb) across a 4.4 Mb region containing the *Myc* locus (chr15: 59,700,000 - 64,100,000). Deposition of H3K4me2/3 as well as Brg1, Ikaros, E2A, EBF1 and Pax5 bound-sites are indicated. The thicknesses of the connecting lines reflect the natural log ratio of observed versus expected interaction frequency in the Hi-C data sets. Bin size used for the analysis was 10 kb. *Myc* gene is highlighted in grey and the distal *Myc* super-enhancer is indicated by a red box. (**e**) Brg1 permits a subset of B-lineage transcription factors access to a super-enhancer to activate *Myc* expression. Brg1, EBF1, Ikaros and Pax5 occupancy in *Rag1*$^{-/-}$ pro-B cells across the super-enhancer (chr15: 63,440,000 - 63,500,000) is shown. Indicated are nucleosome-depleted regions as determined by ATAC reads across the super-enhancer for both *Smarca4*$^{+/+}$ and *Smarca4*$^{\Delta/\Delta}$ pro-B cells. (**f**) Ikaros occupancy across the *Myc* super-enhancer is significantly decreased in Brg1-depleted pro-B cells. Ikaros-bound sites across the *Myc* super-enhancer are indicated in *Smarca4*$^{+/+}$ pro-B cells and Smarca4$^{\Delta/\Delta}$ pro-B cells (Sites 1 and 2 are shown in red in (**e**)). **c**: Average and standard deviation from three

independent experiments. **f**: Representative from two independent experiments. *$P < 0.05$ (two-tailed unpaired Student's *t* test).

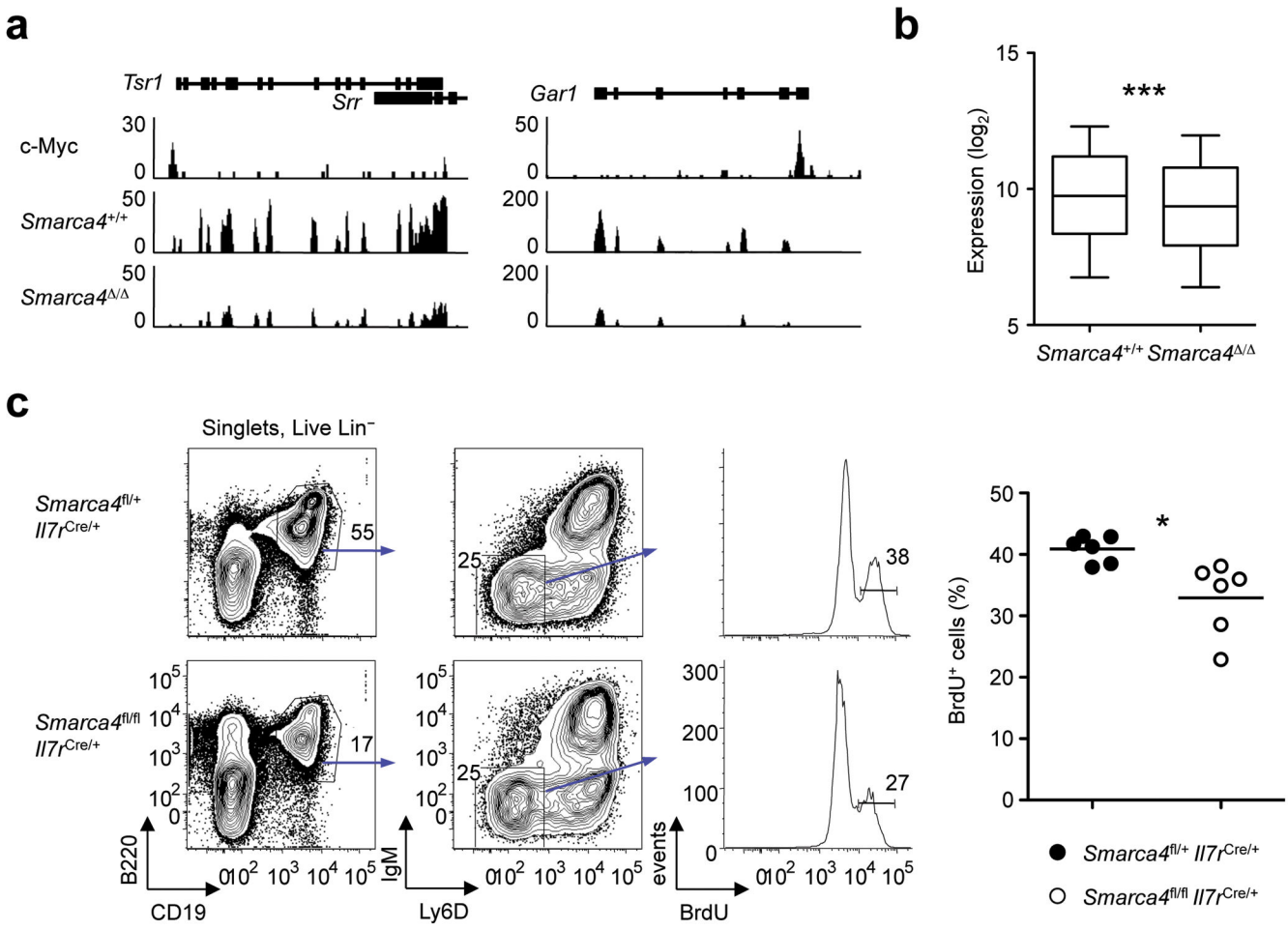

Figure 6.

Brg1 regulates *Myc* expression to promote pro-B cell growth. (**a**) c-Myc occupancy associated with the promoter regions of the *Gar1* and *Tsr1* genes is depicted. Tag counts derived from the RNA-Seq reads derived from *Smarca4*$^{+/+}$ and *Smarca4*$^{\Delta/\Delta}$ pro-B cells are indicated. RNA-Seq tag counts are representative of two independent experiments. (**b**) Relative transcript levels of genes associated with c-Myc occupancy in promoter regions in *Smarca4*$^{+/+}$ and *Smarca4*$^{\Delta/\Delta}$ pro-B cells. ***$P = 1 \times 10^{-38}$ (two-tailed paired Student's *t* test). (**c**) BrdU incorporation in pro-B cells derived from *Smarca4*$^{fl/fl}$*Il7r*$^{Cre/+}$ mice as compared to *Smarca4*$^{fl/+}$*Il7r*$^{Cre/+}$ mice. Mice were sacrificed 4 hours after BrdU injection. Left panels show the gating strategy to identify pro-B cells ($Lin^-Live^+CD19^+B220^+IgM^-Ly6D^-$). Right panel indicates percentage of BrdU incorporation in pro-B cells. Data is derived from two independent experiments. *$P < 0.05$ (two-tailed unpaired Student's *t* test).

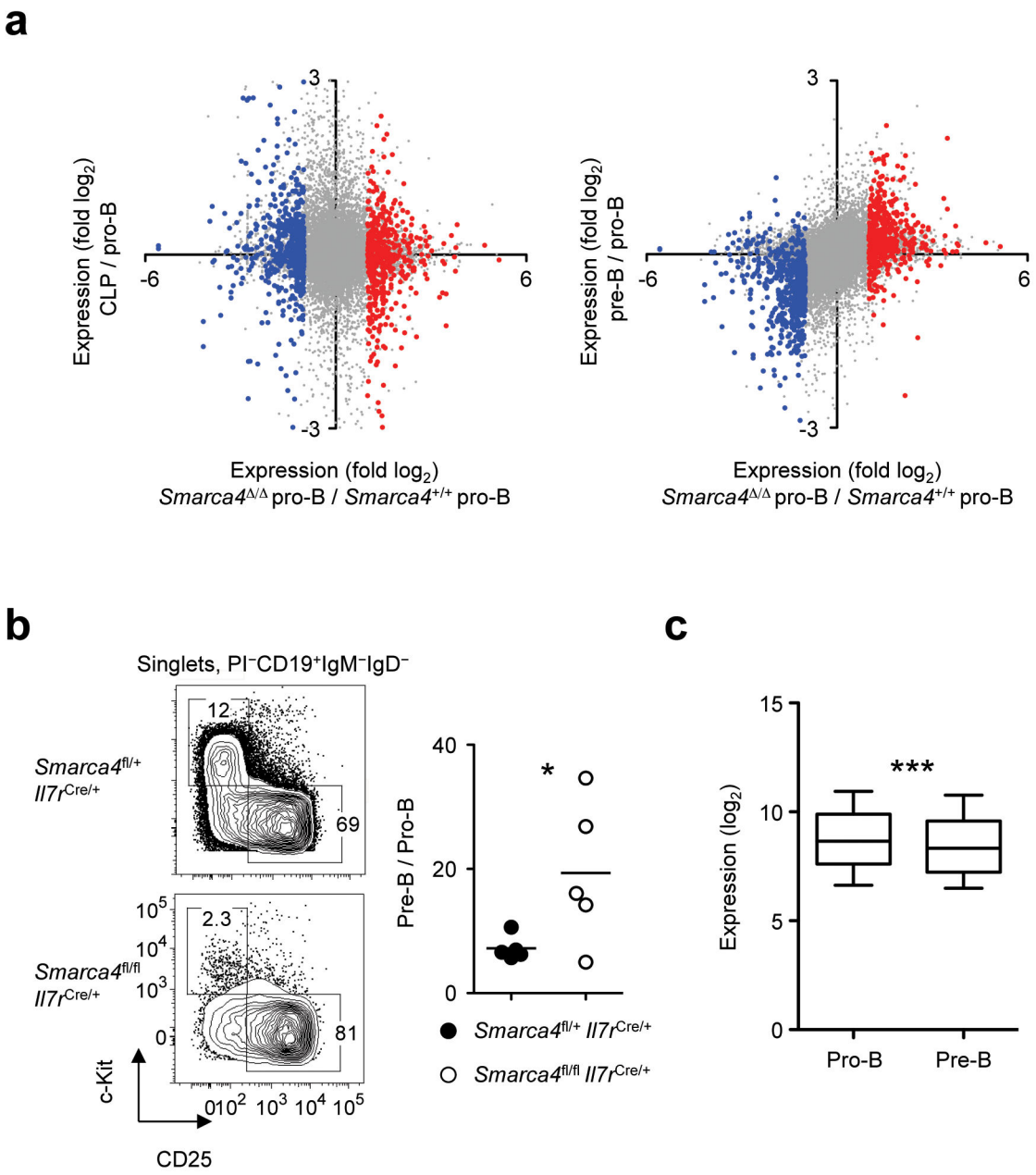

Figure 7.

Brg1 expression acts to maintain the pro-B cell compartment. (**a**) Brg1 acts to suppress the induction of a pre-B lineage specific program of gene expression. Left panel shows changes in transcript abundance in *Smarca4*$^{\Delta/\Delta}$ pro-B cells versus *Smarca4*$^{+/+}$ pro-B cells plotted against changes in transcript abundance in CLPs versus pro-B cells. Spearman correlation = −0.05. Right panel shows changes in transcript abundance in *Smarca4*$^{\Delta/\Delta}$ pro-B cells versus *Smarca4*$^{+/+}$ pro-B cells plotted against changes in transcript abundance in pre-B cells versus pro-B cells. Spearman correlation = 0.37. Transcripts highlighted in blue and red represent significant differences (> 2-fold) between *Smarca4*$^{\Delta/\Delta}$ pro-B cells when compared to *Smarca4*$^{+/+}$ pro-B cells. Gene expression in CLP, pro-B and pre-B cells determined by

microarray by the ImmGen Consortium (**b**) Flow cytometric analysis of the pro-B ($IgM^{-}IgD^{-}Kit^{+}CD25^{-}$) and pre-B ($IgM^{-}IgD^{-}Kit^{-}CD25^{+}$) cell compartments in *Smarca4*$^{fl/+}$*Il7r*$^{Cre/+}$ and *Smarca4*$^{fl/fl}$*Il7r*$^{Cre/+}$ mice. Right panel indicates the ratios of pre-B versus pro-B cells. Representative of 3 independent experiments. (**c**) Transcript expression of genes associated with c-Myc occupancy in pro-B cells and pre-B cells. ***$P = 2 \times 10^{-32}$ (two-tailed paired Student's *t* test).